Scientia Iranica B (2018) 25(2), 772–789

Sharif University of Technology
Scientia Iranica
Transactions B: Mechanical Engineering
http://scientiairanica.sharif.edu

A design approach to coaxial magnetic gear and determination of torque capability

M.A. Rahimi, M. Durali*, and M. Asghari

Department of Mechanical Engineering, Sharif University of Technology, Tehran, Iran.

Received 24 September 2016; received in revised form 6 December 2016; accepted 19 June 2017

KEYWORDS
Magnetic gear;
Mechanical gear;
Design parameter;
Torque capacity;
Gear module.

Abstract. This paper presents a time-saving methodology for the design and sizing of the magnetic gear sets. Some new design parameters similar to mechanical gears were defined to calculate the torque capacity. Finite-element analysis was extensively used to calculate the variation of torque capacity of gear set due to changes in different geometric parameters of a set. Different design curves were obtained by which the design and sizing of the gears can routinely be accomplished. Optimal performance of magnetic gear was not the main target of this research, and utilization of this method helps gear designers to decide on parameters, such as scale of gears, magnet thickness, stack length, and pole pair numbers, and come up with a near-optimum geometry design.

1. Introduction

Magnetic Gear (MG) is more likely to have a bright future in many industries. Having no physical contact between gears, lower noise and vibration, lower maintenance cost, high reliability due to no mechanical failure, and mechanical isolation of input and output are just a few advantages of magnetic gears.

In recent years, magnetic gears have gained more attention due to higher performance and torque intensity in newer topologies. Atallah and Howe [1] presented a novel magnetic gear design with improved torque capability. Based on this methodology, different types of magnetic gears have been presented in recent years, such as linear MG [2], cycloid MG [3], axial field MG [4], harmonic MG [5], and high-speed ratio MG [6]. In addition, much attention has been paid to the application of magnetic gears in different industries. Jian et al. [7] introduced a combination of magnetic gear with permanent magnet machines for wind power generation. Magnetic geared in-wheel motor is designed in [8] which leads to improvement of torque and power densities of motors for electric vehicles. In addition, a new powertrain for hybrid vehicles is introduced in [9] which has an integrated permanent magnet electric motor and a generator with a coaxial magnetic gear.

Different design parameters influence the torque capability of magnetic gears. Design optimization becomes more complicated as some of these parameters are in conflict. Knowing the influence of different parameters on torque capability can help the designer make better decisions. Effects of dimensional parameters have been investigated in some researches. For example, in [10], influence of radial thickness of stationary pole pieces on torque capability for different pole pair numbers was studied. Effect of magnet thickness on a motor integrated magnetic gear was investigated in [11]. Moreover, in [12], effects of many design parameters on torque capability, such as gear ratio, ferromagnetic pieces geometry, and permanent magnet thickness and volume were studied separately.

In designing mechanical gears, parameters, such

*. *Corresponding author. Tel./Fax: +98 21 66165514*
E-mail address: durali@sharif.edu (M. Durali)

doi: 10.24200/sci.2017.4326

as gear module, teeth number, and gear width, determine the overall geometry of a gear. These parameters, along with material specifications, determine torque capability of mechanical gears. For designing MGs, there is no specific formulation to designate a gear based on desired torque capacity and gear ratio. As a result, dealing with a large number of influencing parameters makes the design approach more complicated.

In this paper, a number of main parameters are introduced to which the geometry, gear ratio, and torque capacity of magnetic gear are related. To find the influence of the main parameters on torque capability, maximum static torque of gears is obtained by 3D FEM analysis for different geometry configurations. Gerber and Wang [13] shows that end effects are not considered in 2D analysis, and calculated stall torque has about 10-15% more errors than 3D FEM analysis does. We, therefore, prefer to perform 3D FEM analysis despite its computation costs. Nearly 2400 cases with a wide range of varieties are solved, and influence of these design parameters on design approach is presented.

2. Magnetic gear geometry

Figure 1 shows the geometry of an MG set and its main geometrical dimensions. There are three rotors, named inner, outer, and steel slot pieces. The input and output shafts of magnetic gearbox can be connected to either two of these rotors, or the third rotor can be grounded or kept stationary. Different configurations of these connections lead to different gear ratios between input and output shafts. Generally, in the steady-state condition, the equation between rotational speeds of these rotors will be as follows:

$$P_h\omega_{\text{in}} + P_l\omega_{\text{out}} - N_s\omega_s = 0, \tag{1}$$

where ω_{in}, ω_{out}, and ω_s are the rotational speeds of the high pole number, low pole number, and steel slot pole-piece rotors, respectively; P_h, P_l, and N_s are high-speed pole pair, low-speed pole pair, and steel slot pieces number, respectively, while $N_s = P_h + P_l$. When each of the rotors is kept stationary, its speed will be zero, and the others will determine the speed ratio.

For designing a magnetic gear, all of the parameters and dimensions shown in Figure 1 should be determined. Some of these parameters are related to each other, and some other can be chosen independently. In this approach, 5 main design parameters are defined, and all other dimensions are related to them. The main design parameters are:

- Scaling Factor (SF), which is defined as:

$$\text{SF} \equiv \frac{R_{\text{out}}}{R_0}, \tag{2}$$

  where R_{out} and R_0 are in mm. R_0 is the reference radius; it is set to 50 mm here;
- Magnet Thickness Factor (TF), which is defined as follows:

$$\text{TF} \equiv \frac{t_1}{\text{SF} * t_0}, \tag{3}$$

  where t_1 and t_0 are in mm. t_0 is reference magnet thickness when R_{out} is 50 mm which is chosen as 5 mm;
- Stack length (L);
- High-speed pole pair number (P_h);
- Low-speed pole pair number (P_l).

SF scales all the dimensions, and it is similar to mechanical gear module. Stack length is the same as mechanical gear width, and pole pair numbers are similar gear teeth numbers. TF is an additional parameter to determine the magnet thickness. TF is the ratio of the magnet thickness to the scaled magnet reference thickness. As SF is defined to scale all the

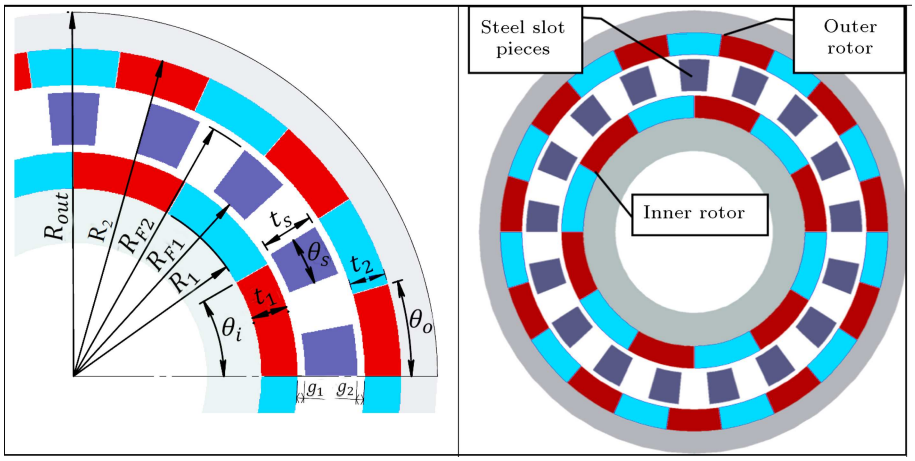

Figure 1. Magnetic gear geometry and dimensions.

Table 1. Dimension of magnetic gear based on design parameters.

No	Parameters
1	$R_2 = \mathrm{SF} * 45$ mm
2	$R_{\mathrm{out}} = R_2 + \mathrm{SF} * 5$ mm
3	$g_1 = g_2 = 1$ mm
4	$t_1 = \mathrm{SF} * \mathrm{TF} * 5$ mm
5	$t_2 = t_1$
6	$\theta_o = 180^\circ / P_l$
7	$\theta_i = 180^\circ / P_h$
8	$\theta_s = 180^\circ / Ns_s$
9	$R_{F2} = R_2 - t2 - g2$
10	$t_s = \pi R_{F2} / N_s$
11	$R_{F1} = R_{F2} - ts$
12	$R_1 = R_{F1} - g1 - t1$

dimensions simultaneously, magnet thickness is also scaled. When TF is fixed, the variation of SF will not change the aspect ratio of the gear. t_0 and R_0 can be any value, and the data are obtained by considering the mentioned values here. In Table 1, correlation of dimensions with the main design parameters is defined.

The two simplifying assumptions to obtain the first solution and geometry of the set are as follows:

1. The thickness and width of ferromagnetic slot pieces are equal, that is:

$$R_{F2}\theta_s = t_s. \tag{4}$$

2. The thickness of magnets of inner and outer rotors is equal:

$$t_1 = t_2. \tag{5}$$

Assumption 1 was made based on the results of [12] in which it is shown that if the ferro thickness-to-pitch ratio is set equal to 0.5, the optimum value of ferromagnetic opening to pitch ratio will be 0.5 to 0.6.

Assumption 2 was also made based on the results of [12] in which, for different volumes of magnets, output torque is nearly at maximum when $t_1 = t_2$. In addition, the difference between the inner and outer PM thicknesses may cause the demagnetization of the thinner PMs, requiring consideration and analysis. Therefore, $t_1 = t_2$ is a suitable assumption. These two assumptions can yield near-optimum value of the torque capacity. As a result, a preliminary design of magnetic gear will be obtained considering these design parameters that will further be fine-tuned to optimize the performance. Airgaps are chosen equal to 1 mm as a usual and normal value for different magnetic machines and gears. The fact is that this parameter has to be fine-tuned in later stages of a magnetic gear design.

Table 2. Material specification of magnetic gears chosen for analysis.

Material	Parameter	Value
Magnet pole	Type	NdFeB-Grade N35
	Remanence [T]	1.21
	Coercivity [kA/m]	890
Ferro slot	Type	Low-carbon steel

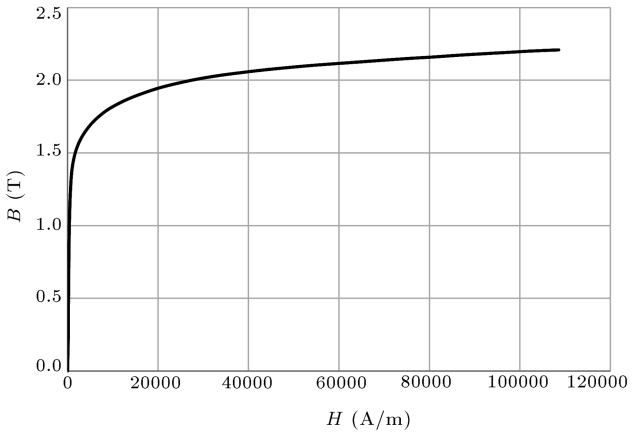

Figure 2. Low carbon steel BH-curve.

Material specification of the MG used for FEM analysis in basic design is listed in Table 2, and low carbon steel BH-curve is shown in Figure 2.

3. Influence of design parameters on magnetic torque capability

Torque capability (T_c) of magnetic gear is defined as follows:

$$Tc \equiv \frac{(T_{\mathrm{in}})_{\max}}{P_h} = \frac{(T_{\mathrm{out}})_{\max}}{P_l} = \frac{(T_s)_{\max}}{N_s}. \tag{6}$$

Moreover, magnetic gear rotor torques can be expressed as follows:

$$T_{\mathrm{in}} = P_h T_C \sin(P_h\theta_{\mathrm{in}} + P_l\theta_o - N_s\theta_s), \tag{7}$$

$$T_{\mathrm{out}} = P_l T_C \sin(P_h\theta_{\mathrm{in}} + P_l\theta_o - N_s\theta_s), \tag{8}$$

$$T_s = -(T_{\mathrm{in}} + T_{\mathrm{out}}), \tag{9}$$

where T_{in}, T_{out}, and T_s are inner, outer, and steel rotor torques, respectively. T_C is torque capability of a magnetic gear that depends on geometry and design parameters. θ_{in}, θ_{out}, and θ_s are inner, outer, and steel rotor rotation angles, respectively. When steel rotor is fixed, θ_s is constant. By multiplying the pole pairs of a rotor and the torque capability of the magnetic gear, maximum torque capacity of the rotor will be obtained.

In this paper, the effect of simultaneous variations of the main parameters on torque capability is studied.

Table 3. Design parameters variation.

Parameter	Values
P_h	2, 4, 6, 8, 10
P_l	11, 15, 19, 25, 29, 35
SF	1, 2, 4, 8, 12
TF	0.25, 0.5, 0.75, 1, 1.25, 1.5, 1.75, 2
L	50, 100

This means that all permutations of variations in each parameter are solved by 3D FEM analysis, and the results are attached in the Appendix. The domains of variations of the main parameters are listed in Table 3.

The specified ranges (extendable by the designer interest) will be useful for designing an MG with a desired specification, and they help reach a good preliminary overall machine size and magnet thickness. In the following, the influence of each design parameter on torque capability is presented, and some points are explained that will help a designer have a better perspective for choosing the parameters ranges.

3.1. Pole pair numbers

Different combinations of pole pair numbers for input and output gears in the specified range generate 30 cases with different gear ratios. It has been attempted to cover the most practical pole pair numbers. The minimum gear ratio between outer and inner gears is:

$$\mathrm{GR}_{\min} = \frac{11}{10} = 1.1,$$

and the maximum gear ratio is:

$$\mathrm{GR}_{\max} = \frac{35}{2} = 17.5.$$

Atallah et al. [10] shows that a harmful effect on transmitted torque of an MG is the cogging torque. Torque ripples are a result of interaction between permanent magnets and ferromagnetic slot pieces.

A cogging torque factor is defined as follows:

$$C_T = \frac{2PN_s}{N_c}, \tag{10}$$

where P is pole pair number of high-speed or low-speed gear, N_s is ferromagnetic pole pieces number, and N_c is the smallest common multiple of $(2P)$ and N_s.

A smaller cogging torque factor results in smaller torque ripple amplitude, which is desirable. To achieve this for a specific gear ratio, pole pair numbers should be chosen so that the smallest common multiple (N_c) has the largest possible value. In this research, low-speed and high-speed pole pair numbers are chosen to have a large N_c for smaller torque ripples.

Herein, the cogging torque is considered as a design suggestion. In fact, in this article, attempt is made to emphasize the important points useful in the design of a magnetic gear based on the results obtained throughout many researches. The main goal is to study the effect of different parameters on static torque and torque capacity of magnetic gears. The dynamic effects will be the subject of future works.

By putting SF = 1, TF = 1, and L = 50 mm and changing the pole pairs, torque capability changes as shown in Figure 3. The maximum inner and outer torques are plotted versus high-speed pole pairs in Figures 4 and 5, respectively. It can be seen that increasing the low-speed pole pairs decreases the torque capability. In addition, it shows that increasing the high speed or decreasing the low speed pole pairs leads to the increase of the maximum inner torque. Maximum outer torque corresponding to each high-speed pole pair number is different, and it varies by changing the low-speed pole pair numbers. It also shows a peak, meaning that the output torque has a maximum value for a fixed set of SF, TF, and L.

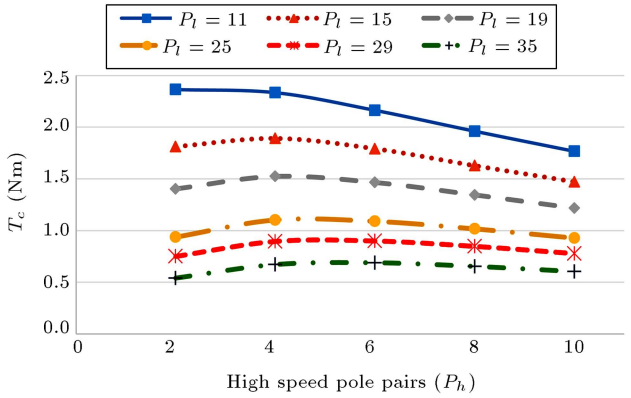

Figure 3. Torque capability of magnetic gear for different pole pair numbers of inner and outer rotor (ST = 1, TF = 1, and L = 50 mm).

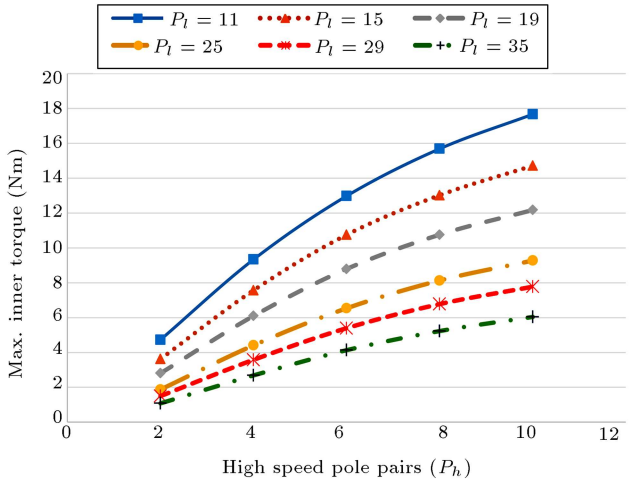

Figure 4. Input torque capacity for different pole pair numbers (ST = 1, TF = 1, and L = 50 mm).

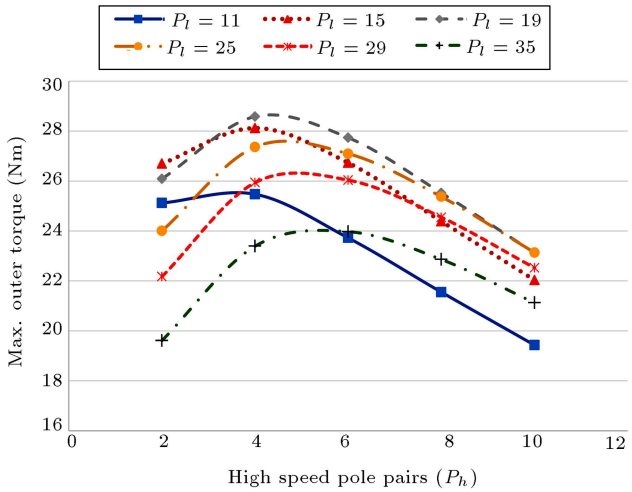

Figure 5. Output torque capacity for different pole pair numbers (ST = 1, TF = 1, and $L = 50$ mm).

3.2. Scaling factor

In this section, variation of torque capability is studied by fixing the pole pair numbers and varying the scaling factor SF. This parameter, which scales the magnetic gear dimensions, can change the peak of outer torque capacity and torque capability.

Fixed design parameters in this section are: TF = 1 and $L = 50$ mm. Figure 6 shows the variation of torque capability versus that of scaling factor for $P_h = 2$ and $P_l = 15$. It is observed that torque capability is a quadratic function of scaling factor by fixing all other design parameters.

The results for different low-speed pole pair numbers and $P_h = 4$ are presented in Figure 7. It can be seen that quadratic torque functions change significantly by varying the low-speed pole pairs. In Figure 8, variation of T_c versus that of scaling factor for high-speed pole pairs $P_l = 15$ is shown. On the contrary, the variations of quadratic functions are not as large as the case for low-speed pole pair numbers.

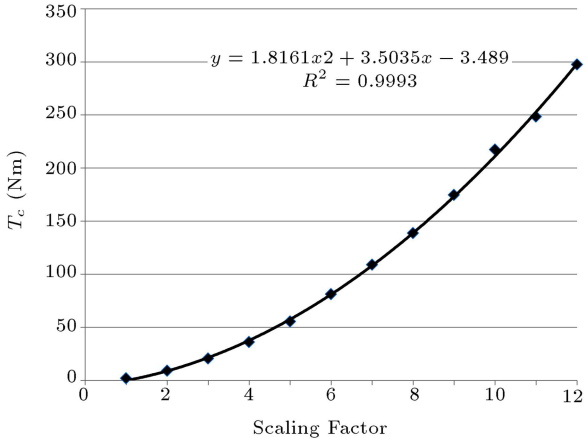

Figure 6. Torque capability of magnetic gear for different scaling factors with $P_h = 2$ and $P_l = 15$.

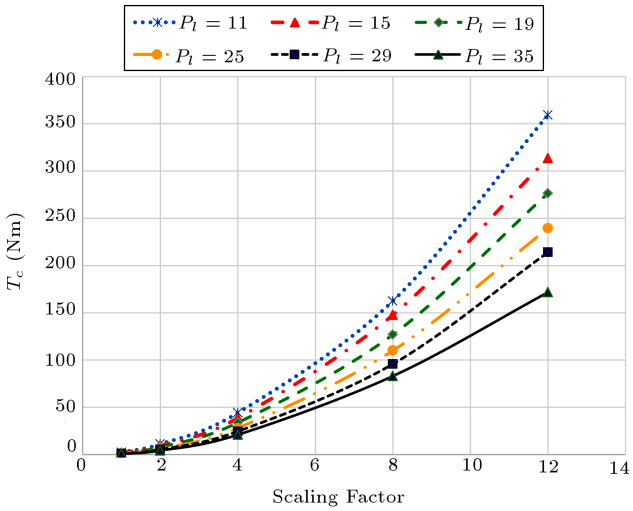

Figure 7. Torque capability versus scaling factor for different low speed pole pair numbers and $P_h = 4$, TF = 1, and $L = 50$ mm.

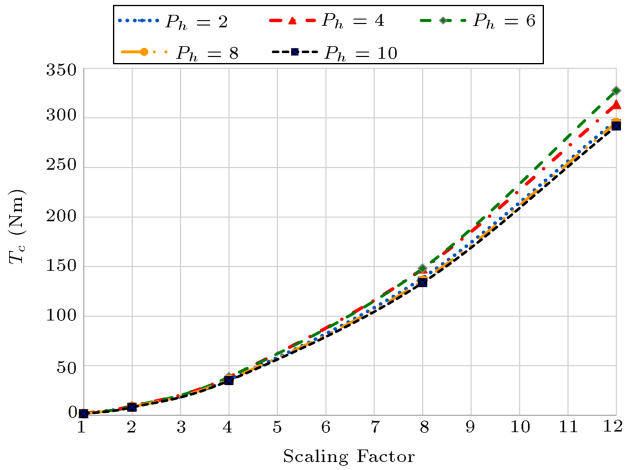

Figure 8. Torque capability versus scaling factor for different high speed pole pair numbers and $P_l = 15$, TF = 1, and $L = 50$ mm.

3.3. Magnetic thickness

One of the important parameters in an MG is the permanent magnet thickness. It affects the torque capability and price of a magnetic gear set. The magnet thickness depends on Scaling Factor (SF) and Thickness Factor (TF). For studying the effect of thickness individually, all other design parameters are fixed and TF is changed.

In Figure 9, variation of torque capability versus that of TF is presented for different low-speed pole pairs while $P_h = 8$, SF = 1, and $L = 50$ mm. Results for different high-speed pole pairs are presented in Figure 10 where $P_l = 25$. Similar results for other values of pole pair numbers and scaling factors are presented in the appendix. The important result is that the torque capability is close to its maximum value when $0.75 < \text{TF} < 1$.

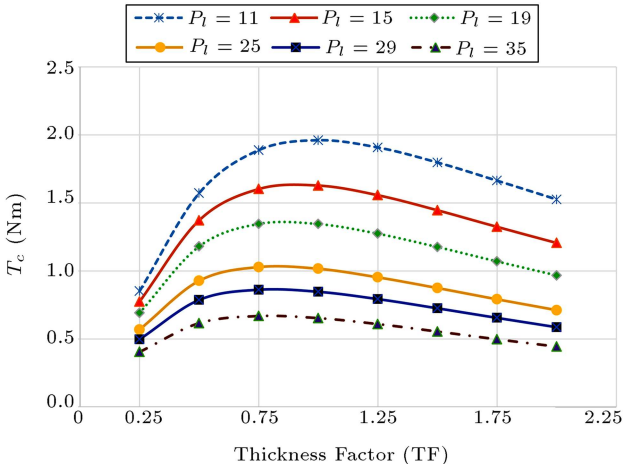

Figure 9. Torque capability versus thickness factor for different low speed pole pairs, $P_h = 8$, SF = 1, and $L = 50$ mm.

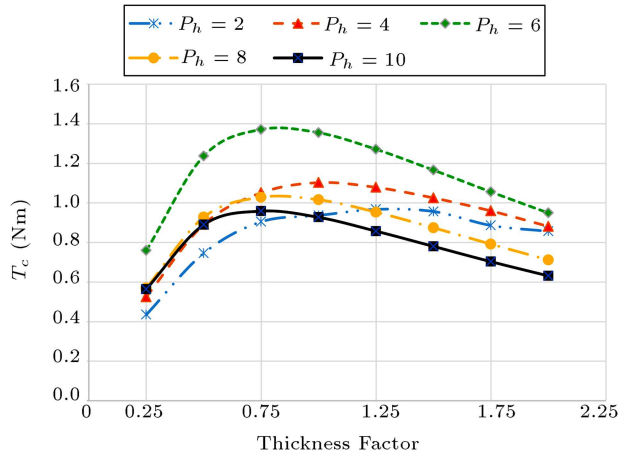

Figure 10. Torque capability versus thickness factor for different high speed pole pairs, $P_l = 25$, SF = 1, and $L = 50$ mm.

3.4. Gear length

Another design parameter to be determined is the magnetic gear stack length. Torque capability for different lengths and different pole pair numbers is displayed in Figure 11, showing a linear behavior.

3.5. Magnetic gear's aspect ratio

In mechanical gears as a rule of thumb, the face width of spur gear is taken between 8 to 12 times of the gear module. In magnetic gears, aspect ratio is defined as in Eq. (11):

$$\text{Aspect ratio} = \frac{L}{2R_{\text{out}}}. \tag{11}$$

For a desired output torque and gear ratio, different aspect ratios can lead to different magnet volumes. Magnets are the most expensive material used in an MG. The minimum volume of magnet for a specific torque capacity (T_c) is investigated by fixing pole pair

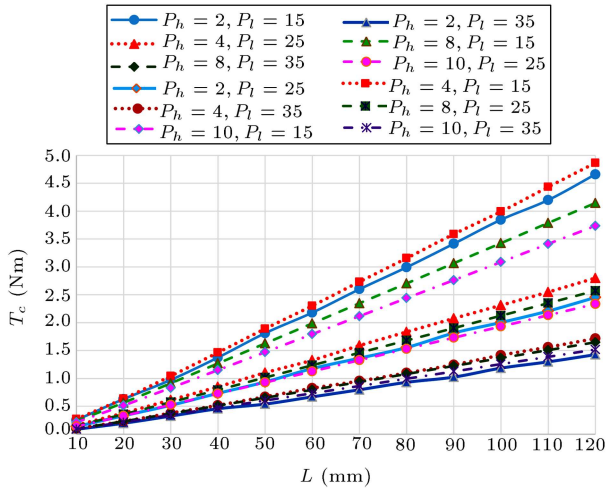

Figure 11. Torque capability for different magnetic gear length and pole pair numbers.

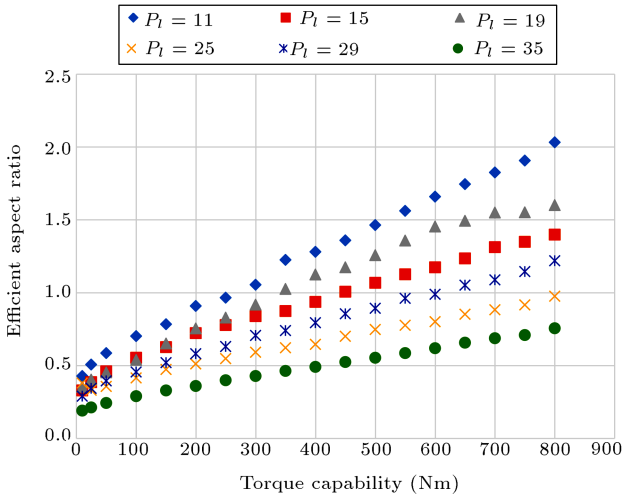

Figure 12. Efficient aspect ratio for different ranges of torque capability and different pole pair numbers (values of efficient aspect ratio for different P_h is averaged).

numbers and changing SF and L. The results of torque capacity are calculated by interpolation between the data in the Appendix. Efficient aspect ratios of gears, which minimize the magnet volume for different pole pair numbers and different torque capacities, are shown in Figure 12. The results show that the most efficient aspect ratios are between 0.5 and 2. In addition, it can be seen that the value of efficient aspect ratio increases for higher torque capability.

3.6. The back iron thickness of inner and outer rotors

The back iron of inner and outer rotors should be thick enough to accommodate all the magnetic flux, which can result in maximum torque capability. In addition, the magnetic flux density in back iron section should be less than saturation level for the iron. Oversizing the back iron beyond the necessary thickness will not

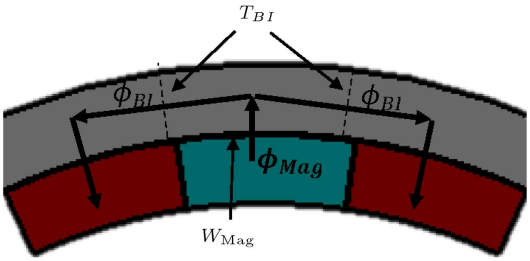

Figure 13. Magnetic flux in magnets mounted on the back iron.

change the torque capability, but decrease the torque density by increasing the magnetic gear volume. Therefore, finding a suitable value of thickness is important.

In Figure 13, magnetic flux in a section of the magnets mounted on the back iron is shown. For obtaining the minimum necessary thickness of the back iron, it is assumed that all flux, entering the back iron through the mounting surface of the magnet, flows through the back iron section toward the neighbor magnets, and no flux escapes from the back iron. By considering the symmetric condition, it results in the following:

$$\phi_{\mathrm{Mag}} = 2\phi_{BI} \rightarrow B_{\mathrm{Mag}} W_{\mathrm{Mag}} = 2B_{BI} T_{BI}, \tag{12}$$

where ϕ_{Mag}, ϕ_{BI}, B_{Mag}, B_{BI}, W_{Mag}, and T_{BI} are magnet flux in the mounting surface, back iron magnetic flux through the thickness, magnet flux density, back iron magnetic flux density, magnet width, and back iron thickness, respectively. If the magnetic flux density in the back iron be lower than $B_I(\max)$, the knee point of B-H curve of low carbon iron should be as follows:

$$\frac{B_{\mathrm{Mag}} W_{\mathrm{Mag}}}{2T_{BI}} \leq B_I(\max). \tag{13}$$

B_0 is considered the maximum value for magnet flux density, and then, from Eq. (13), thickness of back iron will be as follows:

$$T_{BI} \geq \frac{B_0 W_{\mathrm{Mag}}}{2B_I(\max)}. \tag{14}$$

By inputting the typical values of the maximum magnet and maximum iron flux densities as $1.2T$ and $1.8T$, respectively, into the equation, it will result in:

$$T_{BI} \geq \frac{1}{3} W_{\mathrm{Mag}}. \tag{15}$$

Magnet widths for inner and outer rotors in magnetic gears are:

$$W_{\mathrm{Mag}}(\mathrm{Inner}) = \frac{\pi R_1}{P_h},$$

and:

$$W_{\mathrm{Mag}}(\mathrm{Outer}) = \frac{\pi R_2}{P_l}, \tag{16}$$

where R_1 and R_2 are the back iron radii in the mounting surface of magnets for inner and outer rotors, respectively, that are shown in Figure 1. Therefore:

$$T_{\mathrm{BI}}(\mathrm{Inner}) \geq \frac{R_1}{P_h},$$

and:

$$T_{\mathrm{BI}}(\mathrm{Outer}) \geq \frac{R_2}{P_l}, \qquad \frac{\pi}{3} \approx 1, \tag{17}$$

when SF = 1, the rotors' radii are $R_1 = 16$ mm and $R_2 = 45$ mm. Between different pole pair numbers considered in this paper, minimum pole pairs are $P_h = 2$ and $P_l = 11$. Thus, when SF = 1, the minimum necessary thickness for back iron will be as follows:

$$T_{\mathrm{BI}}(\mathrm{Inner}) \geq \frac{16}{2} = 8 \text{ mm},$$

and:

$$T_{\mathrm{BI}}(\mathrm{Outer}) \geq \frac{45}{11} = 4.1 \text{ mm}. \tag{18}$$

The back iron thicknesses are considered the same for different pole pair numbers for simplicity, and the values for inner and outer rotors are set as 10 mm and 5 mm, respectively, when SF = 1. By increasing SF, the back iron thickness will also be scaled. The back iron thickness should be fine-tuned and can be reduced as the pole pair numbers are increased.

4. A design approach to magnetic gear

The basic specifications of a magnetic gear set, such as gear ratio, maximum torque, and dimension constraints, should be decided first. Then, the design process continues as follows.

4.1. Design torque determination

In mechanical gear design, design load is obtained by multiplying correction and overload factors and increasing the maximum working load in order to avoid failure of gear under normal operating conditions:

$$T_{\mathrm{des}} = K_o * K_m * T_L, \tag{19}$$

where K_o and K_m are overload and manufacturing correction factors, respectively. K_o depends on the type of load and the source of input power. In designing mechanical gears, K_o is used to prevent unexpected tooth fracture due to overloads. In magnetic gears, K_o is applied to account for undesirable slippage occurring as a result of overloads, which may cause dynamic effects and loss of drive-train control. Slippage makes

Table 4. Overload correction factor, K_o.

Source of power	Driven machinery		
	Uniform	Moderate sock	Heavy shock
Uniform	1.00	1.25	1.75
Light shock	1.25	1.50	2.00
Medium shock	1.50	1.75	2.25

the system jerky and may cause instability of input or output shafts. Value K_o defined for mechanical gears [14] is presented as a reference to show the severity of excess load exerted on the gear under shock condition. At this point, the designers, according to their application, must decide if they want to protect the drivetrain against the shock in all situations or need to digest the shocks by slippage. These values are listed in Table 4.

K_m can be used as a correction factor to compensate for the errors between manufactured prototypes and the results of FEM design. It can also lead to safe margins for preventing slippage in a normal operation. References [10,13,15,16] have reported up to 30% error between prototype and FEM analysis results. These deviations are the result of flux leakage and airgap tolerances with respect to axial gear length.

In addition, Eqs. (7) and (8) present torque versus relative rotational angles. There is only one point at which the maximum torque can be obtained. If the gear operates at its maximum torque capability as a nominal value, then the magnetic gear will encounter slippage by a small change of relative angle between input and output rotors. Next, the maximum torque capability is chosen 20% higher than the gear set nominal torque. As a result of up to 13% variation in a relative angle between input and output shafts, the torque will not pass the maximum torque capability.

Therefore, a logical value for K_m can be considered between 1.2 and 1.4 to compensate for these deviations.

4.2. Choosing scaling factor and length

Considering the design torque, other design parameters, such as scaling factor, length, and pole pair numbers, should be chosen properly. As mentioned before, output torque has a peak value when SF and L are fixed and pole pair numbers are changed. Maximum output torque of gears for a given SF and L can be calculated by interpolation of appendix data.

In Table 5, the peak of output torque for different scaling factors and typical lengths of $L = 50$ mm and 100 mm are presented when $P_h \in [2 \text{ to } 10]$ and $P_l \in [11 \text{ to } 35]$. This table shows the min values of SF and L for a specific desired output torque. To obtain the maximum output torque for different lengths, a linear

Table 5. Maximum output torque for different SF and $L = 50$ mm-100 mm, TF = 1.

SF	$2R_{\text{out}}$ (mm)	P_h	P_l	Max T_o (Nm)	
				$L = 50$ (mm)	$L = 100$ (mm)
1	100	5	18	29	57
1.5	150	5	28	96	190
2	200	5	29	165	327
2.5	250	6	35	321	636
3	300	6	35	483	956
3.5	350	6	35	645	1277
4	400	6	35	808	1600
5	500	6	35	1417	2806
6	600	6	35	2025	4010
7	700	6	35	2634	5215
8	800	6	35	3243	6421
9	900	6	35	4226	8367
10	1000	6	35	5208	10312
11	1100	6	35	6191	12258
12	1200	6	35	7173	14203

interpolation can be used as follows:

$$T_{O_{\max}}(L) = \frac{T_{o_{(L=100\ \text{mm})}} - T_{o_{(L=50\ \text{mm})}}}{50} * (L - 50) + T_o(L = 50\ \text{mm}). \quad (20)$$

L can be chosen to have an efficient aspect ratio as mentioned before. For initial value, L can be selected proportional to SF as follows:

$$0.5 * \text{SF} * 100\ \text{mm} < L < 2 * \text{SF} * 100\ \text{mm}. \quad (21)$$

4.3. Choosing pole pair numbers

After choosing SF and L, pole pair numbers should be specified to meet the desired objects. By choosing P_h, P_l is calculated based on desired gear ratio:

$$P_l = P_h * \text{GR}_o. \quad (22)$$

By choosing the pole pair numbers, all the design parameters are determined and torque capability can be calculated by interpolation of appendix data. Then, output torque will be obtained by:

$$T_{\text{outer}} = P_l * T_c. \quad (23)$$

If applying this trial-and-error process to choose the pole pair numbers does not bring about an acceptable result, SF and L should be revised. In choosing pole pair numbers, minimization of cogging torque factor (C_T), which is explained before, should also be taken into account. The exact desired gear ratio may not be obtained if cogging factor is to be minimized.

Table 6. Preferred thickness for magnets.

mm	1	1.5	2	3	4	5	6	8	10	15	20
inch	1/32	1/16	3/16	1/8	1/4	3/8	1/2	3/4	1	2	3

4.4. Finalizing the dimensions and FEM analysis

Fine-tuning of some dimensions may be required at the final stage of design. One of the effective dimensions is the magnets thickness. The thicknesses of magnets in inner and outer rotors are assumed equal ($t_1 = t_2$). They can be different and should be fine-tuned for minimum magnet volume based on common magnet thicknesses. The common thicknesses for magnets are listed in Table 6.

When dimensions are finalized, FEM analysis on the final model can be done to validate the interpolated data.

5. Data verification

For verification of the data, two sets of prototypes are investigated. These prototypes are shown in Figures 14-16. The design parameters, such as P_l, SF, TF, and L, are the same in these prototypes, and rectangular shaped magnets are used instead of arc type magnets. Here, the outer ring is fixed and output shaft is coupled with ferromagnetic rotor.

Torque capability of gears is estimated by interpolation of the appendix data. The design parameters, calculated torque, and experimental results for two gear sets are listed in Table 7.

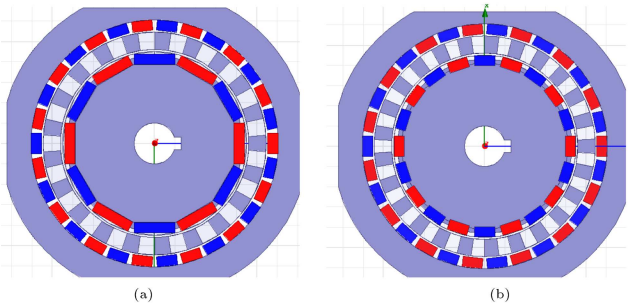

Figure 14. Designed magnetic gears: (a) Gear set 1 and (b) gear set 2.

Figure 15. Inner rotors and slot pieces of 2 sets of magnetic gear.

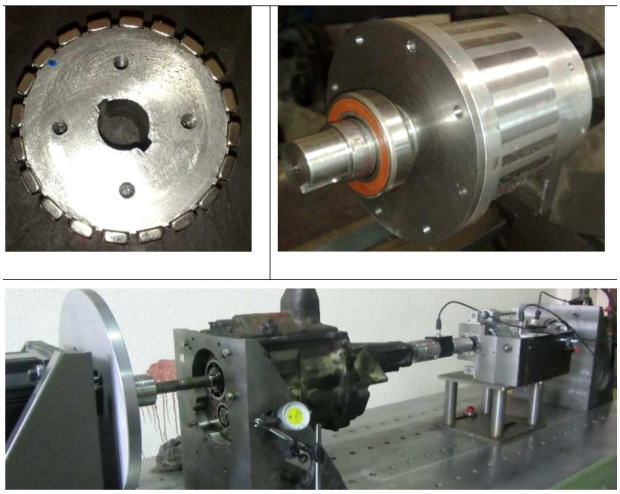

Figure 16. Parts of magnetic gear sets and test setup.

Table 7. Design parameters of 2 magnetic gear sets and calculated torque.

No.	Design parameters	Gear set 1	Gear set 2
1	R_{out}	60	60
2	t_1	5	5
3	P_h	6	10
4	P_l	15	15
5	L	50	50
6	SF	1.2	1.2
7	TF	0.83	0.83
8	Max (T_s) Calculated from proposed method	59	60
9	Max (T_s) Experimental results	48.0	46.3
10	Error	18.5%	22.8%

The difference between experimental results and calculated torques is acceptable. It should be noted that rectangular shape of magnet pieces results in the larger difference.

FEM analysis of the fine-tuned models has been done to clarify the effects of rectangular shape magnets and other tolerances. FEM analyses and experimental results for two sets are presented in Figures 17 and 18.

Table 8. Comparison of max. low speed rotor torque from references' results with calculated torque from the proposed method.

No.	Design parameters	References				
		[13]	[17]	[18] CMGRM	[19] CMGRM	[20]
1	R_{out}	65	60	107	72	78
2	t_1	5	5	8	5.5	5
3	P_h	2	4	4	4	3
4	P_l	21	22	17	22	31
5	L	40	15	40	100	10
6	SF	1.3	1.2	2.2	1.4	1.6
7	TF	0.77	0.83	0.73	0.79	0.64
8	Max (T_{out}) from proposed method	45.2	10.1	142	135.0	10.7
9	Max (T_{out}) Ref. FEM results	44.2	10.5	139.7	134.5	9.5
10	Max (T_{out}) Ref. experimental results	33.5	8.0	137.0	—	9.5
11	No 8 & 9 Error	2.2%	3.7%	1.6%	0.4%	11.1%
12	No 8 & 10 Error	25.9%	21.4%	3.5%	—	11.7%

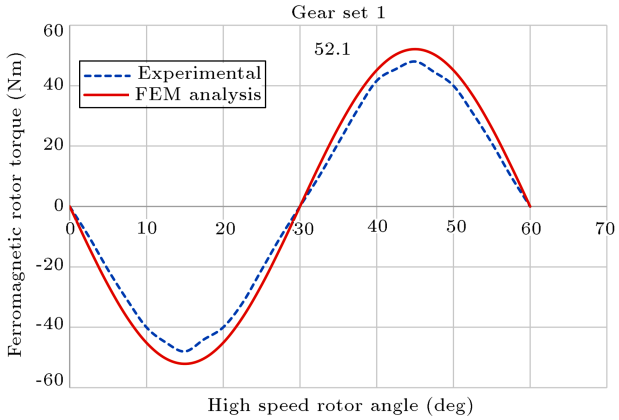

Figure 17. FEM analysis of output torque of magnetic gear set 1 by the comparison of experimental results.

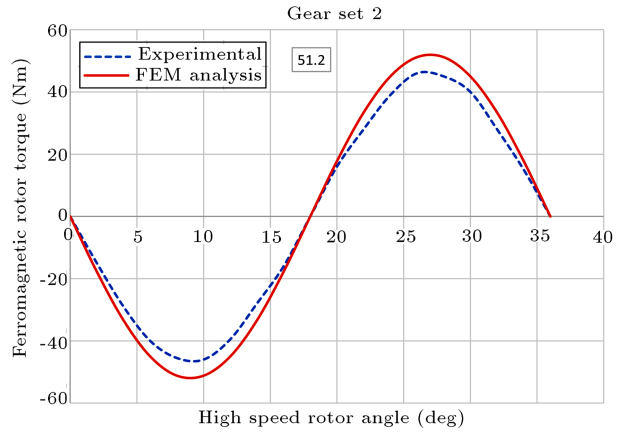

Figure 18. FEM analysis of output torque of magnetic gear set 2 by the comparison of experimental results.

Output torque difference of the fine-tuned model and the proposed method calculation is 12% in gear set 1 and 13% in gear set 2. Difference of the experimental results with the final FEM analysis is 8.5% for gear set 1 and 12.3% for gear set 2.

For more validity, some of FEM and experimental results of magnetic gearboxes, which are presented in different references, are surveyed, and the calculation method is applied. Based on the magnetic gear dimensions noted in the references, the main design parameters (SF, TF, P_h, P_l, and L) are determined. By knowing the design parameters, static torque calculations of the gears are done from Appendix data and results are listed in Table 8.

By comparing the calculated torque and references results, it can be seen that a good compromise exists. The results were then evaluated in two different aspects:

FEM analysis on the final model shows up to 12% difference in output torque capacity with the estimation from the proposed method. This shows that the proposed method and defined main parameters can result in a good preliminary design for the gear sets.

In addition, the results show that up to 25% difference between FEM and experimental results may exist. These errors between analytical and experimental results have often been reported for magnetic gears in different references [10,13,15,16]. The manufacturing tolerances, mechanical mounting, material specifications, and airgap tolerances lead to this difference. As a result, it was suggested in this article that if one is to use the generated data and current method

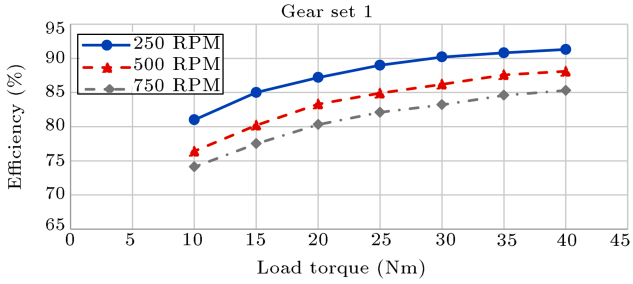

Figure 19. Variation of efficiency with transmitted torque on steel slot pieces for different inner rotor speeds in gear set 1.

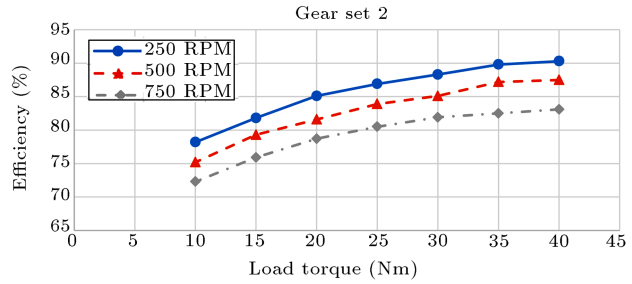

Figure 20. Variation of efficiency with transmitted torque on steel slot pieces for different inner rotor speeds in gear set 2.

for obtaining a close-to-exact design, correction factor, k_m, is to be employed based on the experience and evaluated cases.

The performance curves of gear sets 1 and 2 in different speeds and torques are shown in Figures 19 and 20. It can be seen that, in higher speeds, the efficiency will be decreased because of iron losses. In addition, in the range of torques lower than maximum torque capability, efficiency is lower. This is because of frictions and mounting losses. Keeping this in mind, the dynamic output torque will obviously be lower than the gear set static torque. This paper is focused on magneto-static torque of the set, and the dynamic performance of gear is to be studied in future work.

6. Conclusion

In this paper, a systematic design approach to the determination of magnetic gear dimensions was devised. Similar to mechanical gears, some main design parameters were defined by which magnetic gear dimensions were determined. The influence of design parameters on torque capability was investigated simultaneously. It was shown that these design parameters could simplify the design approach. The method can very well determine a preliminary design of the gears, and accordingly, torque capability of the set can be calculated further by interpolation of appendix data. The data and results obtained in this paper, which are presented for a wide range of effective parameter variations, can be a good starting point for formation of a magnetic gear design handbook. The data presented here give the gear designers a tool for comparing mechanical and magnetic gear solutions. The proposed method was validated by comparing experimental and FEM analysis results of some magnetic gear sets with the results obtained from this method. The results seem to be very promising and time saving in magnetic gear design.

Acknowledgment

The authors would like to thank Shahid Rezaee Advanced Research Institute for the award of the research grant for this work.

References

1. Atallah, K. and Howe, D. "A novel high-performance magnetic gear", *IEEE Transactions on Magnetics*, **37**, pp. 2844-2846 (2001).
2. Atallah, K., Wang, J., and Howe, D. "A high-performance linear magnetic gear", *Journal of Applied Physics*, **97**, pp. 1-3 (2005).
3. Joergensen, F.T., Andersen, T.O., and Rasmussen, P.O. "The cycloid permanent magnetic gear", In *Conference Record - IAS Annual Meeting (IEEE Industry Applications Society)*, Tampa, FL, pp. 373-378 (2006).
4. Mezani, S., Atallah, K., and Howe, D. "A high-performance axial-field magnetic gear", *Journal of Applied Physics* 99, 08R303, pp. 1-3 (2006).
5. Rens, J., Atallah, K., Calverley, S.D., and Howe, D. "A novel magnetic harmonic gear", In *Proceedings of IEEE International Electric Machines and Drives Conference, IEMDC 2007*, Antalya, pp. 698-703 (2007).
6. Man, Y., Zhao, Y., Bian, C., Wang, S., and Zhao, H. "A kind of magnetic gear with high speed ratio", In *Proceedings-3rd International Conference on Information Sciences and Interaction Sciences, ICIS 2010*, Chengdu, pp. 632-634 (2010).
7. Jian, L.N., Chau, K.T., Dong, Z., Jiang, J.Z., and Zheng, W. "A magnetic-geared outer-rotor permanent-magnet brushless machine for wind power generation", In *Industry Applications Conference, 2007. 42nd IAS Annual Meeting. Conference Record of the 2007 IEEE*, pp. 573-580 (2007).
8. Chau, K.T., Zhang, D., Jiang, J.Z., Liu, C., and Zhang, Y. "Design of a magnetic-geared outer-rotor permanent-magnet brushless motor for electric vehicles", *IEEE Transactions on Magnetics*, **43**, pp. 2504-2506 (2007).
9. Jian, L., Xu, G., Wu, Y., Cheng, Z., and Song, J. "A novel power-train using coaxial magnetic gear for power-split hybrid electric vehicles", In *2011 Interna-*

tional Conference on Electrical Machines and Systems, ICEMS 2011, Beijing (2011).

10. Atallah, K., Calverley, S.D., and Howe, D. "Design, analysis and realisation of a high-performance magnetic gear", *IEE Proceedings: Electric Power Applications*, **151**, pp. 135-143 (2004).
11. Rasmussen, P.O., Mortensen, H.H., Matzen, T.N., Jahns, T.M., and Toliyat, H.A. "Motor integrated permanent magnet gear with a wide torque-speed range", In *2009 IEEE Energy Conversion Congress and Exposition, ECCE 2009*, San Jose, CA, pp. 1510-1518 (2009).
12. Evans, D.J. and Zhu, Z.Q. "Influence of design parameters on magnetic gear's torque capability", In *2011 IEEE International Electric Machines and Drives Conference, IEMDC 2011*, Niagara Falls, ON, pp. 1403-1408 (2011).
13. Gerber, S. and Wang, R.J. "Evaluation of a prototype magnetic gear", In *Industrial Technology (ICIT), 2013 IEEE International Conference on*, pp. 319-324 (2013).
14. Dudley, D., Chief Editor, *Gear Handbook*, Ed., McGraw-Hill Book Co (1962).
15. Jorgensen, F.T., Andersen, T.O., and Rasmussen, P.O. "Two dimensional model of a permanent magnet spur gear-A mathematical method used to model a parallel magnetised magnetic spur gear", In *Conference Record - IAS Annual Meeting (IEEE Industry Applications Society)*, Kowloon, Hong Kong, pp. 261-265 (2005).
16. Li, Y., Xing, J.W., Lu, Y.P., and Yin, Z.J. "Torque analysis of a novel non-contact permanent variable transmission", *IEEE Transactions on Magnetics*, **47**, pp. 4465-4468 (2011).
17. Shah, L., Cruden, A., and Williams, B.W. "A magnetic gear box for application with a contra-rotating tidal turbine", In *Proceedings of the International Conference on Power Electronics and Drive Systems*, Bangkok, pp. 989-993 (2007).
18. Jian, L., Chau, K.T., Gong, Y., Jiang, J.Z., Yu, C., and Li, W. "Comparison of coaxial magnetic gears with different topologies", *IEEE Transactions on Magnetics*, **45**, pp. 4526-4529 (2009).
19. Li, X., Chau, K.T., Cheng, M., Hua, W., and Du, Y. "An improved coaxial magnetic gear using flux focusing", In *2011 International Conference on Electrical Machines and Systems, ICEMS 2011*, Beijing (2011).
20. Fukuoka, M., Nakamura, K., and Ichinokura, O. "A method for optimizing the design of SPM type magnetic gear based on reluctance network analysis", In *Electrical Machines (ICEM), 2012 XXth International Conference on*, pp. 30-35 (2012).

Appendix

Torque capability resulting from 3D FEM analysis for different design parameters (SF, TF, L, P_h, and P_l) is presented in Table A.1. One can use these data for designing a new magnetic gear. T_c is torque capability.

Table A.1. 3D FEM result for different design parameters.

T_c (Nm)		$P_h = 2$, $P_l = 11$		$P_h = 4$, $P_l = 11$		$P_h = 6$, $P_l = 11$		$P_h = 8$, $P_l = 11$		$P_h = 10$, $P_l = 11$	
		L									
SF	**TF**	**50**	**100**	**50**	**100**	**50**	**100**	**50**	**100**	**50**	**100**
1	0.25	0.88	1.81	0.87	1.82	0.87	1.82	0.85	1.77	0.82	1.70
1	0.5	1.63	3.51	1.69	3.57	1.66	3.49	1.57	3.30	1.47	3.08
1	0.75	2.14	4.52	2.14	4.56	2.04	4.32	1.89	3.98	1.73	3.63
1	1	2.36	5.09	2.33	4.97	2.16	4.59	1.96	4.14	1.77	3.72
1	1.25	2.44	5.31	2.36	5.02	2.13	4.54	1.91	4.03	1.70	3.58
1	1.5	2.42	5.27	2.28	4.88	2.03	4.32	1.80	3.80	1.59	3.36
1	1.75	2.33	5.06	2.14	4.59	1.88	4.01	1.66	3.51	1.47	3.10
1	2	2.19	4.76	1.98	4.25	1.74	3.68	1.53	3.22	1.35	2.84
2	0.25	5.17	10.8	4.85	10.5	4.94	10.5	4.90	10.5	4.81	10.2
2	0.5	8.64	18.5	8.50	18.6	8.49	18.5	8.25	18.0	7.90	17.1
2	0.75	10.5	22.9	10.3	23.1	10.1	22.2	9.58	21.0	9.03	19.7
2	1	11.4	25.2	11.1	24.7	10.5	23.3	9.88	21.7	9.18	20.1
2	1.25	11.6	26.1	11.2	25.0	10.4	23.1	9.61	21.2	8.90	19.5
2	1.5	11.3	25.7	10.7	24.3	9.9	22.1	9.13	20.1	8.42	18.4
2	1.75	10.9	24.7	10.3	22.9	9.3	20.8	8.55	18.8	7.89	17.2
2	2	10.4	23.4	9.5	21.2	8.7	19.3	7.96	17.5	7.33	16.0
4	0.25	24.3	51.0	20.8	48.5	22.6	50.6	22.8	50.4	22.5	49.9

Table A.1. 3D FEM result for different design parameters (continued).

T_c (Nm)		$P_h = 2$, $P_l = 25$		$P_h = 4$, $P_l = 25$		$P_h = 6$, $P_l = 25$		$P_h = 8$, $P_l = 25$		$P_h = 10$, $P_l = 25$	
		L									
SF	**TF**	**50**	**100**	**50**	**100**	**50**	**100**	**50**	**100**	**50**	**100**
4	0.5	37.6	86.3	35.3	80.6	35.7	81.5	35.1	80.0	34.0	77.4
4	0.75	44.5	100	42.1	96.0	41.0	95.2	39.5	91.3	37.8	87.1
4	1	46.2	108	44.2	104	42.7	98.7	40.3	93.6	38.1	88.2
4	1.25	47.2	112	43.7	103	41.8	97.2	39.1	91.3	37.0	85.6
4	1.5	47.0	109	43.3	100	39.9	93.2	37.4	87.0	35.1	81.3
4	1.75	44.6	104	41.1	96	37.3	87.9	35.3	81.8	33.1	76.6
4	2	42.2	98	37.9	88	35.3	82.3	33.0	76.6	31.0	71.7
8	0.25	101	217	88.5	193	92.3	208	92.0	211	91.5	209
8	0.5	145	330	134	307	135	318	134	314	130	303
8	0.75	173	390	156	367	156	360	149	348	142	335
8	1	179	413	163	381	157	372	150	354	142	336
8	1.25	190	420	170	386	154	362	145	342	138	326
8	1.5	191	414	160	380	149	349	139	327	131	311
8	1.75	179	400	153	353	140	330	131	310	124	294
8	2	167	382	144	328	131	308	123	291	116	276
12	0.25	225	486	191	431	201	455	205	462	201	459
12	0.5	323	734	298	670	294	677	291	669	281	651
12	0.75	372	875	337	768	337	763	323	734	306	707
12	1	394	886	359	826	344	788	325	748	307	707
12	1.25	400	896	366	821	337	760	316	717	296	688
12	1.5	414	877	359	782	323	729	301	686	283	655
12	1.75	401	840	333	736	305	694	283	651	266	617
12	2	372	798	313	708	285	651	266	613	250	581
1	0.25	0.69	1.44	0.76	1.58	0.79	1.64	0.77	1.61	0.75	1.56
1	0.5	1.30	2.74	1.42	2.97	1.43	3.00	1.37	2.87	1.30	2.71
1	0.75	1.65	3.46	1.76	3.73	1.72	3.63	1.60	3.37	1.47	3.09
1	1	1.81	3.85	1.89	3.99	1.79	3.78	1.63	3.43	1.47	3.09
1	1.25	1.81	3.92	1.88	4.01	1.74	3.69	1.56	3.28	1.39	2.92
1	1.5	1.81	3.86	1.81	3.86	1.64	3.46	1.45	3.04	1.29	2.69
1	1.75	1.74	3.76	1.69	3.61	1.51	3.19	1.32	2.79	1.17	2.46
1	2	1.61	3.54	1.55	3.32	1.38	2.91	1.21	2.53	1.07	2.23
2	0.25	4.17	8.57	4.43	9.46	4.73	10.0	4.62	9.82	4.64	9.84
2	0.5	6.85	14.9	7.52	16.3	7.73	16.8	7.50	16.2	7.32	15.7
2	0.75	8.18	18.3	8.85	19.6	8.98	19.6	8.50	18.5	8.11	17.6
2	1	9.01	19.8	9.40	21.0	9.25	20.3	8.59	18.8	8.09	17.6
2	1.25	9.15	19.9	9.48	20.8	9.00	19.9	8.28	18.1	7.71	16.8
2	1.5	8.77	19.7	8.95	20.1	8.54	18.8	7.78	17.0	7.22	15.7
2	1.75	8.63	18.9	8.51	19.1	7.94	17.6	7.24	15.8	6.71	14.5
2	2	8.24	18.2	8.04	17.6	7.33	16.2	6.68	14.5	6.19	13.4
4	0.25	19.1	44.5	20.6	45.6	22.4	49.8	21.9	48.2	22.6	49.7
4	0.5	30.7	66.5	32.3	71.9	34.2	77.2	32.7	74.0	32.7	73.8
4	0.75	35.6	77.0	36.8	84.5	38.0	87.7	36.1	82.6	35.4	80.9

Table A.1. 3D FEM result for different design parameters (continued).

T_c (Nm)		$P_h = 2$, $P_l = 15$		$P_h = 4$, $P_l = 15$		$P_h = 6$, $P_l = 15$		$P_h = 8$, $P_l = 15$		$P_h = 10$, $P_l = 15$	
		L									
SF	**TF**	**50**	**100**	**50**	**100**	**50**	**100**	**50**	**100**	**50**	**100**
4	1	36.0	82.5	38.7	88.4	38.7	89.9	36.3	83.4	35.0	80.3
4	1.25	37.5	84.8	37.6	90.1	37.6	87.1	34.9	80.4	33.5	76.9
4	1.5	35.4	83.7	36.8	85.9	36.0	82.9	32.9	75.8	31.6	72.3
4	1.75	34.3	82.3	35.3	81.8	33.7	77.9	30.8	71.0	29.6	67.4
4	2	34.4	75.8	33.4	76.5	31.5	72.3	28.7	66.0	27.6	62.7
8	0.25	76.9	178	85.2	192	92.4	212	89.7	204	94.3	215
8	0.5	110	265	124	279	132	306	126	293	128	300
8	0.75	128	291	142	334	147	342	136	321	136	320
8	1	139	329	148	337	148	345	136	321	134	317
8	1.25	143	320	150	340	145	335	131	309	128	303
8	1.5	141	329	137	333	136	320	124	293	121	287
8	1.75	141	304	134	309	128	302	116	276	113	269
8	2	130	290	130	287	120	281	108	258	106	252
12	0.25	164	421	167	406	204	472	198	448	209	482
12	0.5	242	598	262	611	284	672	272	628	278	644
12	0.75	289	640	315	694	314	735	294	680	295	684
12	1	297	673	314	721	327	727	295	681	292	677
12	1.25	319	705	319	718	312	714	283	654	278	646
12	1.5	303	675	298	709	304	682	268	621	263	613
12	1.75	305	685	292	667	279	646	252	584	246	576
12	2	295	624	275	620	260	598	235	544	230	539
1	0.25	0.59	1.23	0.66	1.38	0.69	1.43	0.69	1.43	0.67	1.40
1	0.5	1.07	2.18	1.18	2.47	1.22	2.55	1.18	2.47	1.12	2.33
1	0.75	1.25	2.68	1.43	3.01	1.43	3.00	1.35	2.82	1.24	2.59
1	1	1.40	2.91	1.52	3.18	1.46	3.09	1.34	2.82	1.22	2.55
1	1.25	1.40	3.00	1.48	3.17	1.41	2.99	1.27	2.67	1.14	2.38
1	1.5	1.39	2.98	1.44	3.04	1.32	2.78	1.18	2.46	1.04	2.18
1	1.75	1.32	2.86	1.34	2.86	1.21	2.56	1.07	2.24	0.95	1.98
1	2	1.25	2.72	1.23	2.62	1.10	2.32	0.97	2.03	0.85	1.78
2	0.25	3.54	7.75	3.96	8.44	4.21	8.90	4.26	9.04	4.24	8.98
2	0.5	5.73	12.4	6.55	14.0	6.75	14.6	6.71	14.4	6.51	14.0
2	0.75	6.92	15.0	7.72	16.5	7.77	16.8	7.49	16.2	7.11	15.3
2	1	7.44	15.9	7.89	17.4	7.85	17.3	7.50	16.3	6.99	15.1
2	1.25	7.39	16.1	7.86	17.6	7.66	16.8	7.15	15.6	6.62	14.3
2	1.5	7.24	16.2	7.56	16.8	7.28	15.9	6.70	14.5	6.16	13.3
2	1.75	6.93	15.3	7.11	15.9	6.75	14.8	6.20	13.5	5.69	12.2
2	2	6.53	14.6	6.56	14.9	6.22	13.6	5.70	12.4	5.23	11.2
4	0.25	17.5	37.2	17.9	40.7	20.2	44.8	20.6	45.2	20.6	45.3
4	0.5	25.4	56.4	28.3	64.0	30.2	67.8	30.0	67.6	29.4	65.9
4	0.75	27.5	65.2	32.5	73.7	33.3	76.1	32.7	74.3	31.4	71.3
4	1	31.5	69.3	33.8	77.1	34.1	77.4	32.5	74.2	30.8	70.1
4	1.25	33.5	72.0	33.7	77.8	32.8	75.5	31.1	71.2	29.3	66.7

Table A.1. 3D FEM result for different design parameters (continued).

T_c (Nm)		$P_h = 2$, $P_l = 19$		$P_h = 4$, $P_l = 19$		$P_h = 6$, $P_l = 19$		$P_h = 8$, $P_l = 19$		$P_h = 10$, $P_l = 19$	
		L									
SF	**TF**	**50**	**100**	**50**	**100**	**50**	**100**	**50**	**100**	**50**	**100**
4	1.5	32.0	67.6	32.1	74.3	31.2	71.7	29.3	67.1	27.6	62.5
4	1.75	30.9	68.0	31.4	71.0	29.3	67.4	27.4	62.6	25.7	58.1
4	2	27.7	63.3	29.3	65.6	27.2	62.5	25.5	58.1	23.9	53.9
8	0.25	76.1	159	73.7	177	83.9	191	85.2	194	85.3	195
8	0.5	117	242	110	253	116	271	116	270	114	267
8	0.75	119	253	126	289	130	299	125	295	120	284
8	1	128	276	127	293	129	304	123	291	118	279
8	1.25	120	280	135	302	125	294	119	280	112	266
8	1.5	129	272	124	286	122	280	112	265	106	251
8	1.75	110	265	117	274	114	265	106	248	99	234
8	2	109	250	115	257	106	247	98	232	92	218
12	0.25	172	349	161	381	184	418	187	429	187	431
12	0.5	216	528	242	559	251	581	254	580	247	577
12	0.75	241	564	268	611	280	644	270	630	259	606
12	1	261	602	276	630	285	649	271	622	254	594
12	1.25	263	592	292	654	274	628	259	598	242	567
12	1.5	275	591	273	618	262	605	242	568	228	533
12	1.75	256	555	260	603	249	567	228	529	215	501
12	2	242	552	248	555	233	521	214	495	199	470
1	0.25	0.43	0.88	0.53	1.06	0.56	1.15	0.57	1.18	0.56	1.16
1	0.5	0.75	1.56	0.89	1.84	0.94	1.96	0.93	1.93	0.89	1.85
1	0.75	0.90	1.87	1.05	2.20	1.07	2.25	1.03	2.15	0.96	2.00
1	1	0.94	2.00	1.10	2.31	1.09	2.29	1.02	2.13	0.93	1.93
1	1.25	0.97	2.04	1.08	2.28	1.05	2.20	0.95	2.00	0.86	1.79
1	1.5	0.96	2.02	1.03	2.18	0.97	2.05	0.87	1.83	0.78	1.63
1	1.75	0.89	1.95	0.96	2.05	0.89	1.88	0.79	1.66	0.70	1.47
1	2	0.86	1.84	0.88	1.87	0.80	1.69	0.71	1.49	0.63	1.31
2	0.25	2.62	5.51	3.34	7.01	3.60	7.63	3.72	7.85	3.77	7.95
2	0.5	4.19	8.9	5.21	11.3	5.59	11.9	5.63	12.0	5.54	11.8
2	0.75	5.16	10.7	6.15	13.0	6.27	13.5	6.14	13.3	5.92	12.7
2	1	5.20	11.4	6.38	13.6	6.35	13.8	6.08	13.2	5.76	12.4
2	1.25	5.19	11.7	6.17	13.5	6.15	13.4	5.81	12.6	5.42	11.6
2	1.5	5.25	11.3	5.91	13.2	5.76	12.7	5.41	11.7	5.02	10.8
2	1.75	5.13	11.1	5.55	12.4	5.38	11.7	4.98	10.8	4.62	9.9
2	2	4.76	10.9	5.20	11.4	4.95	10.8	4.57	9.9	4.23	9.1
4	0.25	11.9	25.2	17.3	35.2	18.0	39.2	18.6	40.5	19.2	41.9
4	0.5	17.8	40.0	24.2	52.1	25.6	57.2	26.0	58.4	26.3	58.4
4	0.75	19.7	47.3	26.1	61.2	28.6	63.9	28.0	63.3	27.6	62.0
4	1	21.9	47.3	28.0	63.4	28.6	64.6	27.7	62.8	26.8	60.5
4	1.25	22.1	51.7	27.9	62.8	27.8	62.8	26.4	60.0	25.4	57.2
4	1.5	21.9	49.8	26.7	62.1	26.4	60.1	24.9	56.6	23.8	53.4
4	1.75	20.9	49.6	25.9	58.8	24.6	56.1	23.2	52.4	22.1	49.6

Table A.1. 3D FEM result for different design parameters (continued).

T_c (Nm)		$P_h = 2$, $P_l = 25$		$P_h = 4$, $P_l = 25$		$P_h = 6$, $P_l = 25$		$P_h = 8$, $P_l = 25$		$P_h = 10$, $P_l = 25$	
		L									
SF	**TF**	**50**	**100**	**50**	**100**	**50**	**100**	**50**	**100**	**50**	**100**
4	2	20.0	46.4	24.1	53.9	22.8	51.9	21.6	48.6	20.5	45.9
8	0.25	46.7	107	70.1	151	75.8	167	78.0	178	82.0	187
8	0.5	65	164	93.3	211	102	240	104	240	106	246
8	0.75	79	170	104	237	112	256	110	257	110	257
8	1	81	188	110	249	112	262	109	254	107	249
8	1.25	84	186	107	247	108	251	104	244	101	237
8	1.5	88	183	105	247	104	239	99	229	95	222
8	1.75	73	170	101	231	97	226	92	214	89	207
8	2	76	178	95.3	218	92	211	86	201	83	194
12	0.25	105	239	145	330	162	374	171	392	183	420
12	0.5	136	331	207	477	221	512	226	523	230	542
12	0.75	168	374	232	535	240	549	238	555	239	559
12	1	194	418	239	548	246	557	237	548	232	542
12	1.25	189	374	243	541	241	543	226	530	221	519
12	1.5	203	386	240	541	228	516	213	497	206	483
12	1.75	184	376	223	493	213	489	201	464	195	456
12	2	169	404	207	469	203	460	188	436	181	425
1	0.25	0.37	0.78	0.45	0.92	0.48	1.00	0.50	1.03	0.50	1.02
1	0.5	0.61	1.29	0.72	1.53	0.79	1.64	0.79	1.64	0.76	1.58
1	0.75	0.73	1.47	0.86	1.79	0.89	1.87	0.86	1.80	0.81	1.68
1	1	0.75	1.61	0.89	1.87	0.90	1.89	0.85	1.77	0.78	1.62
1	1.25	0.76	1.63	0.88	1.86	0.86	1.81	0.79	1.66	0.72	1.49
1	1.5	0.77	1.60	0.84	1.77	0.80	1.68	0.73	1.52	0.65	1.35
1	1.75	0.72	1.55	0.78	1.66	0.73	1.53	0.66	1.37	0.58	1.21
1	2	0.67	1.46	0.71	1.52	0.65	1.38	0.59	1.22	0.52	1.08
2	0.25	2.44	5.15	2.96	6.09	3.26	6.81	3.37	7.12	3.42	7.19
2	0.5	3.80	7.7	4.47	9.6	4.88	10.5	5.00	10.7	4.93	10.5
2	0.75	4.12	9.1	5.25	11.2	5.48	11.8	5.41	11.7	5.23	11.2
2	1	4.54	9.9	5.40	11.7	5.52	12.0	5.35	11.6	5.08	10.9
2	1.25	4.41	9.6	5.31	11.6	5.34	11.7	5.09	11.0	4.76	10.2
2	1.5	4.50	9.9	5.07	11.2	5.00	11.0	4.74	10.2	4.40	9.4
2	1.75	4.25	9.6	4.81	10.7	4.68	10.1	4.36	9.4	4.04	8.7
2	2	3.84	9.1	4.42	9.8	4.28	9.3	3.99	8.6	3.70	7.9
4	0.25	11.8	26.5	13.8	32.5	16.4	35.7	17.2	37.5	17.6	38.2
4	0.5	17.4	37.5	20.6	47.0	23.2	51.4	23.7	52.8	23.8	52.6
4	0.75	18.9	42.9	23.6	54.7	25.4	57.4	25.4	57.1	24.9	55.5
4	1	18.8	45.6	24.5	55.2	25.7	58.1	25.1	56.7	24.1	54.2
4	1.25	20.1	44.4	23.9	54.9	24.9	56.1	23.9	54.3	22.8	51.2
4	1.5	19.5	46.0	23.8	52.5	23.3	54.1	22.5	50.9	21.4	47.8
4	1.75	20.1	42.7	22.5	51.1	22.0	50.4	21.0	47.3	19.9	44.4
4	2	18.9	43.8	20.6	46.7	20.3	46.5	19.4	43.8	18.4	40.9
8	0.25	46.1	108	67.3	143	68.1	160	73.3	163	74.8	169

Table A.1. 3D FEM result for different design parameters (continued).

T_c (Nm)		$P_h = 2$, $P_l = 29$		$P_h = 4$, $P_l = 29$		$P_h = 6$, $P_l = 29$		$P_h = 8$, $P_l = 29$		$P_h = 10$, $P_l = 29$	
		L									
SF	**TF**	**50**	**100**	**50**	**100**	**50**	**100**	**50**	**100**	**50**	**100**
8	0.5	70	154	90.7	188	94	214	96	221	96	222
8	0.75	75	180	91	218	102	234	102	234	99	230
8	1	72	181	96	225	101	236	100	233	96	225
8	1.25	73	162	100	224	100	230	96	223	91	214
8	1.5	80	180	92	215	95	221	91	210	86	201
8	1.75	70	173	92	207	89	206	85	196	80	187
8	2	74	163	86.9	190	83	191	79	183	75	174
12	0.25	103	250	141	322	151	353	160	367	167	378
12	0.5	136	326	192	421	210	467	210	484	208	486
12	0.75	162	326	202	461	223	509	222	511	215	502
12	1	174	382	214	490	226	519	220	506	209	490
12	1.25	172	407	208	483	216	499	210	486	200	465
12	1.5	171	393	216	471	210	473	199	461	188	440
12	1.75	182	352	199	447	197	442	184	433	176	410
12	2	152	354	192	418	188	424	173	402	163	383
1	0.25	0.35	0.73	0.39	0.80	0.40	0.83	0.41	0.84	0.35	0.73
1	0.5	0.56	1.16	0.61	1.27	0.62	1.28	0.60	1.25	0.56	1.16
1	0.75	0.65	1.35	0.68	1.42	0.67	1.39	0.63	1.31	0.65	1.35
1	1	0.67	1.42	0.69	1.44	0.65	1.37	0.60	1.26	0.67	1.42
1	1.25	0.66	1.39	0.65	1.37	0.61	1.28	0.55	1.15	0.66	1.39
1	1.5	0.62	1.32	0.61	1.27	0.55	1.16	0.50	1.04	0.62	1.32
1	1.75	0.58	1.24	0.55	1.16	0.50	1.04	0.45	0.93	0.58	1.24
1	2	0.52	1.12	0.49	1.04	0.44	0.93	0.40	0.82	0.52	1.12
2	0.25	2.48	5.17	2.77	5.84	2.91	6.12	2.99	6.28	2.48	5.17
2	0.5	3.67	7.8	4.05	8.7	4.19	8.9	4.19	8.9	3.67	7.8
2	0.75	3.98	9.0	4.49	9.6	4.53	9.7	4.40	9.4	3.98	9.0
2	1	4.23	9.3	4.55	9.8	4.46	9.6	4.26	9.1	4.23	9.3
2	1.25	4.22	9.3	4.39	9.5	4.23	9.1	3.98	8.5	4.22	9.3
2	1.5	4.07	9.1	4.15	9.1	3.93	8.5	3.68	7.9	4.07	9.1
2	1.75	3.85	8.5	3.83	8.4	3.62	7.8	3.37	7.2	3.85	8.5
2	2	3.55	7.9	3.51	7.6	3.29	7.1	3.07	6.5	3.55	7.9
4	0.25	12.5	26.9	14.6	31.4	15.4	33.2	16.0	34.6	12.5	26.9
4	0.5	17.5	39.5	20.1	44.5	20.8	45.8	20.3	46.7	17.5	39.5
4	0.75	19.4	44.7	22.1	49.1	21.9	49.3	21.8	48.8	19.4	44.7
4	1	21.0	48.5	21.9	49.6	21.9	48.9	21.3	47.6	21.0	48.5
4	1.25	20.6	46.5	21.2	48.2	20.7	46.8	20.1	44.8	20.6	46.5
4	1.5	20.4	45.8	20.3	45.9	19.6	44.0	18.7	41.9	20.4	45.8
4	1.75	18.5	42.9	19.0	43.3	18.1	40.8	17.4	38.8	18.5	42.9
4	2	17.4	41.0	17.7	39.4	16.8	37.6	16.1	35.7	17.4	41.0
8	0.25	54.2	122	62.7	141	66.5	149	70.1	158	54.2	122
8	0.5	75.0	171	83	189	86	197	88	203	75.0	171
8	0.75	80	182	91	206	91	211	91	210	80	182

Table A.1. 3D FEM result for different design parameters (continued).

T_c (Nm)		$P_h = 2$, $P_l = 35$		$P_h = 4$, $P_l = 35$		$P_h = 6$, $P_l = 35$		$P_h = 8$, $P_l = 35$		$P_h = 10$, $P_l = 35$	
		L									
SF	**TF**	**50**	**100**	**50**	**100**	**50**	**100**	**50**	**100**	**50**	**100**
8	1	83	190	90	209	89	205	88	204	83	190
8	1.25	86	190	86	201	86	198	83	194	86	190
8	1.5	82	190	84	194	80	188	78	182	82	190
8	1.75	81	175	79	181	76	175	73	169	81	175
8	2	76.6	170	74	167	70	162	68	157	76.6	170
12	0.25	124	266	137	317	148	337	158	362	124	266
12	0.5	153	378	182	415	186	435	193	451	153	378
12	0.75	180	425	186	454	197	457	200	464	180	425
12	1	172	419	196	451	198	451	194	455	172	419
12	1.25	179	414	195	435	189	431	185	430	179	414
12	1.5	181	400	183	419	179	409	172	402	181	400
12	1.75	173	397	176	395	168	387	163	380	173	397
12	2	176	380	163	373	154	360	152	351	176	380

Biographies

Mohammad Amin Rahimi is a PhD Candidate at the Mechanical Engineering Department of Sharif University of Technology. He works on the design of magnetic gears and multi-level magnetic gearboxes. He received BS (2008) and MSc (2010) degrees in Mechanical Engineering from Sharif University of Technology, Tehran, Iran. He is currently the Director of Tosan Ltd., a company which aims to develop electric vehicle powertrain such as magnetic gearboxes and high torque permanent magnet machines.

Mohammad Durali is a Professor at the Mechanical Engineering Department of Sharif University of Technology. He received his PhD (1980) and MSc (1976) degrees from MIT and BSc (1974) from Sharif University of Technology. His Major research activities are system design and automation, system dynamics, and turbomachinery and propulsion. Aside from academic activities, he heads up a large research team working on projects from industry. All his projects are industry funded.

Mohsen Asghari is a Professor in Mechanical Engineering Department of Sharif University of Technology. He received his BSc (2000), MSc (2002), and PHD (2007) degrees in Mechanical Engineering from Sharif University of Technology. His major research activities have been focused on theoretical and mathematical aspects of solid mechanics, particularly continuum mechanics.